SHARP



NACA TN 2853



# NATIONAL ADVISORY COMMITTEE FOR AERONAUTICS

TECHNICAL NOTE 2853

## A STUDY OF THE APPLICATION OF POWER-SPECTRAL METHODS OF GENERALIZED HARMONIC ANALYSIS TO GUST LOADS ON AIRPLANES

By Harry Press and Bernard Mazelsky

Langley Aeronautical Laboratory
Langley Field, Va.

NACA

Washington
January 1953

1M

NATIONAL ADVISORY COMMITTEE FOR AERONAUTICS

TECHNICAL NOTE 2853

# A STUDY OF THE APPLICATION OF POWER-SPECTRAL METHODS OF GENERALIZED HARMONIC ANALYSIS TO GUST LOADS ON AIRPLANES

By Harry Press and Bernard Mazelsky

## SUMMARY

The applicability of some results from the theory of generalized harmonic analysis (or power-spectral analysis) to the analysis of gust loads on airplanes in continuous rough air is examined. The general relations for linear systems between power spectrums of a random input disturbance and an output response are used to relate the spectrum of airplane load in rough air to the spectrum of atmospheric gust velocity. The power spectrum of loads is shown to provide a measure of the load intensity in terms of the standard deviation (root mean square) of the load distribution for an airplane in flight through continuous rough air. For the case of a load output having a normal distribution, which appears from experimental evidence to apply to homogeneous rough air, the standard deviation is shown to describe the probability distribution of loads or the proportion of total time that the load has given values. Thus, for an airplane in flight through homogeneous rough air, the probability distribution of loads may be determined from a power-spectral analysis.

In order to illustrate the application of power-spectral analysis to gust-load analysis and to obtain an insight into the relations between loads and airplane gust-response characteristics, two selected series of calculations are presented. In the first series, the standard deviations of loads in continuous rough air described by an assumed power spectrum are calculated for systematic variations in the frequency and damping characteristics of the airplane response to a step-gust input. The results obtained indicate that the loads in rough air are particularly sensitive to variations in the damping characteristics of the oscillatory response to a step gust and largely independent of variations in the frequency. In the second application, the standard deviation of loads is calculated for selected variations of each of several airplane geometric and aerodynamic parameters of an idealized and stable transport-type airplane. The standard deviations obtained are compared with results derived by conventional techniques of using the calculated peak response to an idealized and representative discrete gust. The results indicate that for stable configurations both methods of analysis yield results that are consistent to a first approximation.

## INTRODUCTION

The study of gust loads on airplanes is a twofold problem requiring the adequate representation of the characteristics of atmospheric turbulence and the determination of the airplane response (loads or motions) in rough air. These problems have been recognized since the inception of gust-load research but because of the difficulties involved only limited approaches to the problems appeared practical. The methods that have been used are described and discussed in detail in reference 1. In general, the approach has been to use simplified airplane-response theory for the determination of the characteristics of discrete gusts from airplane measurements of load. The "gusts" derived on this basis are then used to calculate loads on other airplanes. Although these procedures appear reasonable for transferring loads to similar airplanes, as indicated in the reference, they are of questionable value for airplanes of widely different characteristics (such as, configurations and stability characteristics). These limitations have, however, not proved serious in the past since the transport airplanes which were primarily affected by gust standards appeared, in general, to follow conventional design. Available data indicate that new transport airplanes experienced gust loads which were, in general, compatible with those predicted from past work.

Trends in aeronautics toward higher speed and the development of missiles have served to introduce a widening range of unusual configurations and aircraft stability characteristics. Furthermore, the gust-load design requirements, which formerly were of concern for transport and bomber airplanes only, appear to have become important for other aircraft as well. As a consequence of these developments, the need for more generally applicable techniques, both for the measurements of the characteristics of atmospheric gusts and for the calculation of the gust loads on new airplanes, has become more urgent.

Developments in the theory of generalized harmonic analysis (ref. 2) appear adaptable for extending the analysis of gust loads beyond the discrete-gust case to the case of continuous turbulence. Techniques from generalized harmonic analysis involving the concept of power spectral density have been used for many years in diverse fields, such as in the study of random-noise problems in communications and in the study of small-scale turbulence of wind tunnels. The concept of the power of a random disturbance, which is fundamental to the present study, is defined by analogy to electrical power to be the time average of the square of the disturbance. The portion of the power arising from components having harmonic frequencies between $\omega$ and $\omega + d\omega$ is denoted as the power spectral density. For linear systems, the power-spectral-density functions of a random input disturbance and an output response are related through the frequency-response characteristics of the system.

Attractive features of spectral analysis for the study of gust loads are the possibilities that:

(1) Continuous turbulence can be described in analytic form by a power spectrum rather than by discrete gusts.

(2) The load response of airplanes to continuous rough air can be evaluated.

(3) The desirable response characteristics of an airplane for minimizing gust effects in continuous rough air will become amenable to analysis.

In view of the attractive features of power-spectral-density methods of analysis, an investigation of the applicability and implications of these techniques to gust-load analysis was undertaken and the results obtained are reported herein. In this paper, the concepts and relations of generalized harmonic analysis are defined and their method of application to the gust-load problem is indicated. The applicability of the normal probability distribution for the representation of the probability distribution of loads in continuous rough air is considered. For the case of a normal distribution of loads, the standard deviation (root mean square) of the load history defines the probability distribution of loads. It is indicated that the standard deviation may be determined from load power spectrum; thus the results of a power-spectral analysis permit the determination of the probability distribution of loads. Finally, in order to illustrate the application of power-spectral analysis to gust-load calculations and to obtain an insight into the relation between loads in continuous rough air and airplane characteristics, two applications are presented. In both applications, the power spectrum of atmospheric turbulence obtained from flight measurements (ref. 2) is used to represent the turbulence input. The first application is intended to represent the effects on gust loads of variations in airplane dynamic longitudinal stability. The second application is intended to illustrate the effects on gust loads of variations of some geometric and aerodynamic parameters of an idealized transport airplane. The indicated variations in load intensity are compared with those derived by conventional techniques of using the peak-load response to an idealized discrete gust.

## SYMBOLS

| | |
|---|---|
| $A(\ )$ | response to unit step disturbance |
| $a_t$ | slope of tail lift curve per radian |

| | |
|---|---|
| $a_w$ | slope of wing lift curve per radian |
| $b, k_o$ | parameters of equation (31) |
| $c$ | airplane wing chord, ft |
| $c_t$ | airplane tail chord, ft |
| $I$ | pitching moment of inertia about center of gravity, slug-ft$^2$ |
| $\nu$ | reduced frequency, $\omega c/V$, radians/chord |
| $l_w$ | horizontal distance from center of gravity of airplane to wing aerodynamic center, ft |
| $l_t$ | horizontal distance from center of gravity of airplane to tail aerodynamic center, ft |
| $N$ | number of observations |
| $\Delta n$ | acceleration increment, g |
| $P$ | probability |
| $P(z)$ | cumulative probability distribution of z, equation (28) |
| $s$ | distance, chords |
| $S$ | wing area, sq ft |
| $S_t$ | tail area, sq ft |
| $t$ | time, sec |
| $T$ | arbitrary value of t, sec |
| $T( )$ | frequency-response function with respect to argument, $\omega$, $\Omega$, or $\nu$ |
| $U$ | vertical gust velocity, ft/sec |
| $V$ | airplane true airspeed, ft/sec |
| $W$ | airplane weight, lb |
| $W( )$ | response to unit impulse disturbance |
| $x$ | distance, ft |
| $X$ | arbitrary value of x, ft |

| | |
|---|---|
| $y$ | arbitrary random variable |
| $f(y)$ | probability density function of variable $y$, equation (23) |
| $y(\ )$ | arbitrary function of arguments $t$, $x$, and $s$ |
| $\overline{y^2(t)}$ | average power of $y(t)$, equation (4) |
| $z$ | standardized variable, $\Delta n/\sigma$ |
| $\alpha_3$ | coefficient of skewness, equation (30b) |
| $\alpha_4$ | coefficient of kurtosis, equation (30c) |
| $\sigma$ | standard deviation of specified random variable, equation (24b) |
| $\rho$ | mass air density, slugs/cu ft |
| $\tau$ | time displacements, sec |
| $R(\tau)$ | autocorrelation function, equation (9) |
| $\Phi(\ )$ | power-spectral-density function of an arbitrary disturbance with respect to $\omega$ or $\Omega$ |
| $\Phi_i(\ )$ | power-spectral-density function of a designated input |
| $\Phi_o(\ )$ | power-spectral-density function of a designated output |
| $\Psi(z)$ | normal distribution with mean of 0 and standard deviation equal to 1, equation (27) |
| $\omega$ | circular frequency, radians/sec |
| $\Omega$ | reduced frequency, $\omega/V$, radians/ft |
| $d\epsilon/d\alpha$ | downwash factor |

Subscripts:

| | |
|---|---|
| max | maximum load response to a discrete gust |
| basic | basic airplane configuration |

A bar over a symbol designates the average value of the quantity.

In this analysis, the use of several independent variables $t$, $x$, and $s$ for an arbitrary disturbance $y(\ )$ and their associated frequency arguments $\omega$, $\Omega$, and $\nu$ has been found necessary. In order to designate that the several functions $y(\ )$, $\Phi(\ )$, and $T(\ )$ depend

upon their arguments a circumflex $\hat{}$ and a tilde $\tilde{}$ have been used over the appropriate sets of functions in accordance with the scheme shown in the following table:

| Function | Variable | | |
|---|---|---|---|
| | t, sec | x, ft | s, chords |
| Disturbance | $y(t)$ | $\hat{y}(x)$ | $\tilde{y}(s)$ |
| Frequency argument | $\omega$ | $\Omega$ | $\nu$ |
| Power-spectral-density function | $\Phi(\omega)$ | $\hat{\Phi}(\Omega)$ | $\tilde{\Phi}(\nu)$ |
| Frequency-response function | $T(i\omega)$ | $\hat{T}(i\Omega)$ | $\tilde{T}(i\nu)$ |
| Impulse response | $W(t)$ | $\hat{W}(x)$ | $\tilde{W}(s)$ |
| Step response | $A(t)$ | $\hat{A}(x)$ | $\tilde{A}(s)$ |

## ANALYSIS

### Basic Concepts and Relations of Power-Spectral Analysis

The theory of generalized harmonic analysis is an outgrowth and generalization of harmonic analysis and is largely the work of Norbert Wiener (ref. 3). Accounts of the theory and method of application are also given in references 2, 4, and 5. In order to orient the reader, a brief account of the background, the basic concepts, and the relations is presented.

The theory of harmonic analysis indicates that an arbitrary periodic function can be represented by a Fourier series in the following manner:

$$F(t) = \frac{A_0}{2} + \sum_{n=1}^{\infty}\left(A_n \cos n\omega t + B_n \sin n\omega t\right) \qquad (1)$$

where

$$A_n = \frac{2}{T}\int_0^T F(t) \cos n\omega t \, dt$$

$$B_n = \frac{2}{T}\int_0^T F(t) \sin n\omega t \, dt$$

and $T$ is equal to $2\pi/\omega$ and is the period of the function. In order to apply this technique to nonperiodic phenomena, the limit of equation (1) as $T$ goes to infinity must be considered. For this case of a nonperiodic function, the Fourier series takes the form of the Fourier integral and is given by

$$F(t) = \frac{1}{2\pi}\int_{-\infty}^{\infty} e^{i\omega t} d\omega \int_{-\infty}^{\infty} F(\tau) e^{-i\omega\tau} d\tau \qquad (2)$$

If the second integral on the right is denoted as $G(\omega)$ then equation (2) can be written in the reciprocal form

$$F(t) = \frac{1}{2\pi}\int_{-\infty}^{\infty} G(\omega) e^{i\omega t} d\omega \qquad (3)$$

where

$$G(\omega) = \int_{-\infty}^{\infty} F(\tau) e^{-i\omega\tau} d\tau$$

The Fourier transform pair thus provides reciprocal relations between the time function $F(t)$ and its frequency representation $G(\omega)$. The quantity $G(\omega)\, d\omega$ gives the contribution of those harmonic components of $F(t)$ whose frequencies lie between $\omega$ and $\omega + d\omega$.

A necessary condition for the application of equation (3) is that the integrals involved be convergent. This condition acts as a severe limitation on the applicability of the Fourier integral relations. In many problems, such as noise in an electric circuit or turbulence encountered by an airplane in flight, the disturbance is nonperiodic, persists

for a relatively long period of time, and shows no tendency of dying out. In these cases the required integrals do not converge and, as a consequence, the frequency representation in terms of equations (2) and (3) is not possible directly.

In order to develop a frequency representation which would be applicable to continuing disturbances, the theory of random processes makes use of the concept of a stationary random process. The characteristics of a stationary random process are described in detail in reference 4. Essentially, the assumption is that the underlying mechanism which gives rise to the disturbance does not change in time and that a statistical equilibrium exists. Thus, the statistical characteristics of the distribution are invariant with time and statistical prediction becomes possible. For the case of a stationary random function of time $y(t)$, the mean square $\overline{y^2(t)}$ is defined by

$$\overline{y^2(t)} = \lim_{T \to \infty} \frac{1}{T} \int_0^T \left[y(t)\right]^2 dt \tag{4}$$

The mean square will usually exist and represent a measure of disturbance intensity. Since $\overline{y^2(t)}$ is a quadratic function of $y(t)$, it has been termed the "average power" of $y(t)$ in analogy to electrical power which is proportional to the square of the current. The function $y(t)$ is considered to be composed of an infinite number of sinusoidal components with circular frequencies $\omega$, between 0 and $\infty$. The portion of $\overline{y^2(t)}$ arising from components having frequencies between $\omega$ and $\omega + d\omega$ is denoted herein by $\Phi(\omega)\, d\omega$. The function $\Phi(\omega)$ has been called the power-spectral-density function in the literature. From this definition, $\Phi(\omega)$ has the property that

$$\overline{y^2(t)} = \int_0^\infty \Phi(\omega)\, d\omega \tag{5}$$

The power-spectral-density function of a random variable $y(t)$ is generally defined in the following manner (see for example, ref. 4)

$$\Phi(\omega) = \lim_{T \to \infty} \frac{1}{\pi T} \left| \int_0^T y(t) e^{-i\omega t} dt \right|^2 \tag{6}$$

where the notation $|\ |$ indicates the modulus of the complex quantity.

If $\Phi(\omega)$ is defined in this manner, it has the property that its integral over the limits 0 to $\infty$ is equal to the power $\overline{y^2(t)}$. That this expression for $\Phi(\omega)$ is consistent with the preceding discussion is seen to be plausible from the fact that, for each frequency, $\Phi(\omega)$ is proportional to the square of the amplitude of the component of $y(t)$ at that frequency. Thus, $\Phi(\omega)\,d\omega$ is a measure of the contribution of that frequency to $\overline{y^2(t)}$. It should be mentioned that the definition equation (6) differs in minor detail from that used in reference 2 but agrees substantially with those used in references 4 and 5.

A significant and useful relation for linear systems exists between the power-spectral-density function $\Phi_i(\omega)$ of a random input disturbance and the power-spectral-density function $\Phi_o(\omega)$ of an associated output through the system frequency-response function $T(i\omega)$. The system frequency-response function (or admittance) $T(i\omega)$ is defined such that $T(i\omega)e^{i\omega t}$ is the system response to the sinusoidal input $e^{i\omega t}$. In these terms, the relation between the power-spectral-density functions is given by

$$\Phi_o(\omega) = \Phi_i(\omega)\left|T(i\omega)\right|^2 \tag{7}$$

For a given linear system, the function $T(i\omega)$ may be conveniently obtained from either the unit impulse response or the unit step response, respectively, by means of the following relations:

$$\left.\begin{aligned} T(i\omega) &= \int_0^\infty W(t)e^{-i\omega t}dt \\ T(i\omega) &= i\omega\int_0^\infty A(t)e^{-i\omega t}dt \end{aligned}\right\} \tag{8}$$

where $W(t)$ is the response to a unit impulse and $A(t)$ is the response to a unit step.

Equation (6) may be used to evaluate the power-spectral-density function from observed data. However, in practice, the power-spectral-density function may be determined more conveniently and less tediously

by using a related function, the autocorrelation function $R(\tau)$, defined by

$$R(\tau) = \lim_{T \to \infty} \frac{1}{T} \int_0^{\infty} y(t)\, y(t + \tau)\, dt \tag{9}$$

The autocorrelation function has the symmetrical property $R(\tau) = R(-\tau)$ and is reciprocally related to the power-spectral-density function by the Fourier cosine transformation in the following manner:

$$\left.\begin{aligned} R(\tau) &= \int_0^{\infty} \Phi(\omega) \cos \omega\tau\, d\omega \\ \Phi(\omega) &= \frac{2}{\pi} \int_0^{\infty} R(\tau) \cos \omega\tau\, d\tau \end{aligned}\right\} \tag{10}$$

Reference 4, for example, shows that this definition of the power-spectral-density function is consistent with the preceding definition of equation (6).

## Some Forms of Power-Spectral Relations for Gust Applications

In this section, the method of application to gust loads on airplanes of the aforementioned concepts and relations is considered. Some available information is presented on the frequency-response function $T(i\omega)$ for the gust-load condition and on the power-spectral-density functions for atmospheric turbulence. Finally, for convenience in gust-load applications of power-spectral methods, the functions and relations are presented in terms of distances rather than time. Use is made of the distances $x$ in feet and $s$ in chords and their associated frequency arguments $\Omega$ and $\nu$. These changes of variables are subsequently shown to be particularly appropriate in the gust case because in these terms the power spectrums are independent of airplane forward speed.

If atmospheric turbulence can be considered a stationary random process, then the basic requirement for the application of the foregoing power-spectral concepts and relations is satisfied. Evidence that this assumption is plausible under some conditions exists and is discussed subsequently. On the basis of this assumption, the turbulent-vertical-velocity distribution along a line in space can at an instant in time

be considered to represent a stationary random function of space consisting of an infinite number of harmonics of various frequencies or wave lengths. For this condition of spacial wave lengths, a natural unit for the associated frequencies would appear to be radians per unit distance or radians per foot. The description of the power-spectral-density function of atmospheric turbulence must thus be given basically in terms of units such as radians per foot. However, for an airplane in flight through rough air, consideration of the airplane as penetrating the gusts and experiencing the associated loads in terms of time is frequently convenient. Thus, the power-spectral-density functions of gust velocity and loads experienced by the airplane may be considered expressible in terms of the frequency argument $\omega$ in radians per second used in the preceding section. It is, therefore, permissible to express the relation between the power spectrums of gust velocity and loads or normal acceleration in terms of equation (7) as

$$\Phi_o(\omega) = \Phi_i(\omega)\left|T(i\omega)\right|^2$$

where $\Phi_o(\omega)$ is the power-spectral-density function of airplane normal acceleration, $\Phi_i(\omega)$ is the power-spectral-density function of gust velocity experienced by the airplane, and $T(i\omega)$ is the airplane normal-acceleration response function for a sinusoidal gust velocity input.

The present study is primarily concerned with vertical gust velocity inputs and acceleration increment $\Delta n$ (load factor) outputs. The function $\Phi_i(\omega)$ will have the dimensions of $(\text{ft/sec})^2/\text{radian/sec}$; $\left|T(i\omega)\right|^2$ will be given in $(g/\text{ft/sec})^2$. Consequently, $\Phi_o(\omega)$ will have the dimensions of $g^2/\text{radian/sec}$. In this form, the power-spectral-density functions, having the dimensions of power/radian/sec, refer to a particular airspeed. Before considering the representation of these functions in a form independent of airplane speed, some remarks on the determination of the frequency-response function for the gust-load condition and on available information concerning the power-spectral-density function for atmospheric turbulence appear appropriate.

Frequency-response function.- Experimental methods for determining the frequency-response function of an airplane for a gust velocity disturbance have unfortunately not yet been developed. The frequency-response function for airplanes for a gust disturbance can, however, be estimated by theoretical methods by solution of the airplane equations of motion for a gust disturbance. Methods for the determination of the frequency-response function for a linear system are described in chapter 2 of reference 4, for example. The calculation of the frequency-response

function may sometimes be more conveniently performed by first determining the airplane response to a step gust by methods such as those described in reference 6. The response of a step gust may then be used in equation (8) in order to determine the frequency-response function for a continuous sinusoidal gust input.

Power spectrum of atmospheric turbulence.- The power-spectral-density functions of atmospheric gust velocity have been studied from airplane flight measurements (ref. 2). Measurements of pitching velocity of a B-25 airplane in flight through rough air were used to determine the power-spectral-density function of atmospheric turbulence for four weather conditions. Clementson determined the reduced autocorrelation function $R(\tau)/R(0)$ of pitching velocity and obtained the output power-spectral-density function by taking its Fourier transform. The appropriate frequency-response function as determined from simplified theoretical calculations was then used in equation (7) to obtain the input spectrum. The normalization of the autocorrelation function $R(\tau)$ by dividing through by $R(0)$ is arbitrary and was made on the basis of yielding a pitching-velocity power of 1 $(\text{degree/second})^2$ for the airplane used in that investigation. The normalized power-spectral-density functions of atmospheric turbulence derived in this manner did not vary appreciably between weather conditions; although, as might be expected, the value of $R(0)$ for the pitching velocity output did vary appreciably, and reflected variations in the average power of turbulence with weather condition. On the basis of the results obtained in reference 2, the conclusion was reached that "atmospheric turbulence is a stationary random process that can be statistically described by a single reduced power-spectral-density curve." Although additional tests under a wide variety of atmospheric conditions and the use of other airplanes are needed to verify this conclusion, the spectrum obtained appears to be representative at least of the conditions covered by the tests. The results obtained in reference 2 for the power-spectral-density function of atmospheric turbulence thus provide a turbulence input and are used in subsequent applications in the present study.

The average reduced power-spectral-density function obtained in reference 2 for an airplane true flight speed of 300 feet per second is shown in figure 1. The results shown are corrected for two errors made in reference 2 and pointed out in reference 7. In addition, the results of reference 2 have been divided by $2\pi$ in order to conform to the definition of the power-spectral-density function used herein, equation (6). The power-spectral-density function shown in figure 1 has dimensions of $(\text{ft/sec})^2/\text{radians/sec}$ and applies to an airplane airspeed of 300 feet per second.

Changes in the frequency argument.- As pointed out previously, $\Phi(\omega)$ has the dimension of a power/radian/sec and thus depends upon the airplane forward speed. In order to express the power-spectral-density functions in terms independent of airplane flight speed, the change of variables

$$\left.\begin{aligned}\Omega &= \frac{\omega}{V} \\ x &= Vt\end{aligned}\right\} \tag{11}$$

is introduced. The variable $\Omega$ is a reduced frequency in radians per foot. The variable $x$ is the airplane flight distance in feet. In terms of these variables, the average power of a disturbance $\hat{y}(x)$ is given by

$$\overline{\hat{y}^2(x)} = \lim_{X \to \infty} \frac{1}{X} \int_0^X \left[\hat{y}(x)\right]^2 dx \tag{12}$$

(The use of the circumflex is explained in the section "Symbols.")

If the power-spectral-density function $\hat{\Phi}(\Omega)$ is given by

$$\hat{\Phi}(\Omega) = \lim_{X \to \infty} \frac{1}{\pi X} \left| \int_0^X \hat{y}(x) e^{-i\Omega x} dx \right|^2 \tag{13}$$

then $\hat{\Phi}(\Omega)$ gives the average power of the disturbance arising from components having frequencies between $\Omega$ and $\Omega + d\Omega$. Inasmuch as

$$\int_0^\infty \hat{\Phi}(\Omega)\, d\Omega = \int_0^\infty \Phi(\omega)\, d\omega = \overline{y^2} \tag{14}$$

it follows from equation (11) that

$$\hat{\Phi}(\Omega) = V\Phi(\omega) = V\Phi(V\Omega) \tag{15}$$

As pointed out in reference 7, the power-spectral-density function for atmospheric turbulence representing $\hat{\Phi}_i(\Omega)$ is incorrectly given in reference 2. The power-spectral-density function $\hat{\Phi}_i(\Omega)$ which corresponds

to the function shown in figure 1, was obtained by equation (15) and is shown in figure 2. The resulting power spectrum of atmospheric turbulence is independent of airplane speed and in a limited sense may represent a universal reduced power-spectral-density function of atmospheric turbulence.

The relation between the frequency-response functions for the sinusoidal input $e^{i\omega t}$ and $e^{i\Omega x}$ is now considered. Since for a given airspeed the gusts represented by $e^{i\omega t}$ and $e^{i\Omega x}$ are, from equations (11), the same gusts, the load responses when expressed in terms of time $t$ and distance $x$ will only involve a change of scale. If $\hat{T}(i\Omega)e^{i\Omega x}$ is the airplane load response to the gust $e^{i\Omega x}$, then the frequency-response functions are simply related in the following manner:

$$\hat{T}(i\Omega) = T(i\omega) = T(iV\Omega) \tag{16}$$

The frequency-response function $\hat{T}(i\Omega)$ may be obtained from relations similar to those of equation (8) and given by

$$\left.\begin{aligned} \hat{T}(i\Omega) &= \int_0^\infty \hat{W}(x)e^{-i\Omega x}dx \\ \hat{T}(i\Omega) &= i\Omega \int_0^\infty \hat{A}(x)e^{-i\Omega x}dx \end{aligned}\right\} \tag{17}$$

where $\hat{W}(x)$ and $\hat{A}(x)$ are the response functions of the unit impulse and unit step disturbances, respectively, expressed as a function of flight distance. These response functions are related to $W(t)$ and $A(t)$, respectively, by the relations

$$\hat{W}(x) = \frac{1}{V}W(t)$$

$$\hat{A}(x) = A(t)$$

In terms of the variable $\Omega$, the input-output relation can, from equations (15) and (16), be expressed by the relation

$$\hat{\Phi}_o(\Omega) = \hat{\Phi}_i(\Omega)\left|T(i\Omega)\right|^2 \tag{18}$$

The average power for a given input and output in terms of the frequency $\Omega$ may from equations (14) and (18) be obtained by the relations

$$\overline{\hat{y}^2(x)} = \int_0^\infty \hat{\Phi}_o(\Omega)\, d\Omega = \int_0^\infty \hat{\Phi}_i(\Omega) \left|\hat{T}(i\Omega)\right|^2 d\Omega \tag{19}$$

Another set of variables is useful in the applications of power-spectral analysis to gust loads. This set involved the reduced frequency $\nu$ in radians per chord and the nondimensional distance $s$ in chords. Because of the need for consideration of unsteady aerodynamics in gust-loads analysis, calculated responses to step gust velocity inputs may frequently be given in terms of the nondimensional distance $s$ and the frequency-response function in terms of the reduced frequency $\nu$. These variables $\nu$ and $s$ are related to $\omega$ and $\Omega$ and to $t$ and $x$ in the following manner:

$$\left.\begin{aligned} s &= \frac{Vt}{c} = \frac{x}{c} \\ \nu &= \frac{\omega c}{V} = c\Omega \end{aligned}\right\} \tag{20}$$

If $\tilde{T}(i\nu)e^{i\nu s}$ is the acceleration response to the gust $e^{i\nu s}$, then $\tilde{T}(i\nu)$ may also be obtained from the impulse or step response by the relations

$$\left.\begin{aligned} \tilde{T}(i\nu) &= \int_0^\infty \tilde{W}(s)e^{-i\nu s}ds \\ \tilde{T}(i\nu) &= i\nu \int_0^\infty \tilde{A}(s)e^{-i\nu s}ds \end{aligned}\right\} \tag{21}$$

where $\tilde{W}(s)$ and $\tilde{A}(s)$ are the responses to the impulse and step gust inputs in terms of the variable $s$. These response functions are related to $W(t)$ and $A(t)$, respectively, by the relations

$$\tilde{W}(s) = \frac{c}{V} W(t)$$

$$\tilde{A}(s) = A(t)$$

The frequency-response function $\tilde{T}(i\nu)$ is related to the functions $T(i\omega)$ and $\hat{T}(i\Omega)$ in the following manner:

$$\hat{T}(i\Omega) = \tilde{T}(ic\Omega) = T(iV\Omega) \tag{22}$$

and involves only a change of scale of the frequency axis. These relations are used in the subsequent applications.

## Relation of Power-Spectral-Density Function to Applied Gust Loads

In order to apply the foregoing methods of analysis to the study of gust loads, the power spectral density of loads must be related to the intensities of the actual loads. The power-spectral-density function, which provides a measure of the average power arising from components at various frequencies, does not directly reflect the load intensities since the actual load at a given time represents the combined output at the various frequencies. Thus, it is desirable to relate the power spectrum of loads to specific quantities of concern in load studies, such as the proportion of total time at a given load intensity (probability distribution of load intensity), the number and intensity of peak loads, and other such particular quantities that may be of interest for structural analysis. In the present report, only the relation of the power-spectral-density function to the probability distribution of load is considered and more specifically the significance of the normal distribution for loads is considered.

Probability distribution of output.- When a linear system is exposed to an input varying in a random manner with time, the probability distribution of the system output $y$ can frequently be represented by a normal probability density distribution defined by the relation

$$f(y) = \frac{1}{\sigma\sqrt{2\pi}} e^{-\frac{1}{2}\left(\frac{y-\bar{y}}{\sigma}\right)^2} \tag{23}$$

where $\bar{y}$ and $\sigma$ are the mean and standard deviation and are defined by

$$\bar{y} = \lim_{T\to\infty} \frac{1}{T}\int_0^T y\, dt \tag{24a}$$

$$\sigma = \left[ \lim_{T \to \infty} \frac{1}{T} \int_0^T (y - \bar{y})^2 dt \right]^{1/2} \tag{24b}$$

Investigations of communication problems associated with noise, which has many obvious similarities to turbulence, have shown that normal distributions are frequently encountered. Rice in reference 8 has, for example, shown that for a linear system the shot effect in a vacuum tube gives rise to a noise current which has a normal distribution of current intensity. Investigation of fluid turbulence frequently yields normal distributions of velocity fluctuations. These results appear to be explained by the central limit theorem of probability (ref. 9) which states that, under general conditions, the distribution of the sum of a large number of random variables tends toward a normal distribution.

The theoretical derivation of the probability distribution of loads for an airplane in flight through rough air is mathematically difficult and appears to involve assumptions regarding the nature of turbulence that are, for the present, questionable. However, if the load time history in continuous rough air is considered to be a stationary random function, the time history can be considered to be made up of the sum of a large number of harmonic components with random phases. If the associated power-spectral-density function is relatively uniform (having no sharp peaks), then the load at any given time is the sum of a large number of random variables of roughly the same order of magnitude. These conditions meet the principal requirements for applicability of the central limit theorem and, consequently, it follows from this theorem that the probability distribution of load intensity may tend toward a normal distribution.

Significance of the normality of the distribution of loads.- If the distribution of airplane acceleration increment in continuous rough air is normal with a zero mean value, the probability density distribution of the acceleration increment $\Delta n$ is completely described by the standard deviation and from equation (23) is given by

$$f(\Delta n) = \frac{1}{\sigma\sqrt{2\pi}} e^{-\frac{1}{2}\left(\frac{\Delta n}{\sigma}\right)^2} \tag{25}$$

Equation (25) is termed the probability density function of $\Delta n$, and $f(\Delta n)\, d(\Delta n)$ can be considered to represent the proportion of total time (or total flight distance) that $\Delta n$ has a value between $\Delta n$ and $\Delta n + d(\Delta n)$.

In order to examine the properties of equation (25), it is convenient to consider the distribution of the variable

$$z = \frac{\Delta n}{\sigma} \tag{26}$$

where $z$ is the so-called standardized variable and has the probability density distribution

$$\Psi(z) = \frac{1}{\sqrt{2\pi}} e^{-z^2/2} \tag{27}$$

The function $\Psi(z)$ is the normal distribution with a mean of zero and a standard deviation equal to 1 and is the error function commonly tabulated. The probability that a random value of $z$ will exceed a given value is given by the integral of equation (27) as follows:

$$P(z) = \int_z^\infty \Psi(z)\, dz \tag{28}$$

Equation (28) defines the cumulative probability distribution of the reduced variable $z$ and in the case of time-history data may be considered to represent the proportion of total time that the value of $z$ exceeds a given value. For a fixed value of probability $P$, $z$ is fixed and can be obtained from tabulations of the integral of the error function. Thus, for example, for $P = 0.00275$, $z = 2$.

Equation (28) indicates that the probability of exceeding a given value of $z$ is a function of only the given value. Conversely for a given value of probability, the largest value of $z$ exceeded is also fixed and depends only upon the probability. Making the substitution $z = \frac{\Delta n}{\sigma}$ into equation (28) yields the result that the probability of exceeding a given value of $\Delta n/\sigma$ is likewise a function only of the value of $\Delta n/\sigma$ and is given by $P\left(\frac{\Delta n}{\sigma}\right)$. The converse also applies that,

for a given value of probability, the largest value of $\Delta n/\sigma$ exceeded is fixed and depends upon the probability. Consequently, the largest value of $\Delta n$ exceeded with a given probability depends upon the value of $\sigma$ and is given by $\sigma z$. The largest value of $\Delta n$ exceeded with a given probability is thus seen to be directly proportional to the standard deviation. For example, when the standard deviation is doubled, the largest value of $\Delta n$ exceeded with a given probability is also doubled. This direct relationship between the value of the standard deviation and the load probability distribution makes the standard deviation an important and significant measure of the load experience for the case of gust loads having a normal distribution. Because of this direct relation between the standard deviation and the load probability distribution, the standard deviation will be useful as a measure of load intensity in the present study.

The foregoing discussion has served to establish the plausibility of gust loads having a normal distribution under some conditions and the significance of the standard deviation of loads for the case of a normal distribution. The standard deviation of loads can be derived from a power-spectral analysis in the following manner: From its definition (eq. (24b)), the standard deviation of load increment output having a zero mean value is the square root of the average power. Thus, the power-spectral-density function of loads and the standard deviation of the probability distribution of loads are related. The standard deviation $\sigma$ may thus be obtained directly from the power-spectral-density functions by the relation

$$\sigma^2 = \int_0^\infty \Phi_o(\omega)\, d\omega = \int_0^\infty \hat{\Phi}_o(\Omega)\, d\Omega \qquad (29)$$

This relation between the probability distribution and power-spectral-density function for the case of a normally distributed output ties the power spectrum to a basic characteristic of the load history and is thus of importance for applications to gust-load analysis.

## APPLICATION TO GUST-LOAD PROBLEMS

In view of the simple relations between the loads and the power-spectral-density functions for the case of normal distributions of loads, the determination of the normality of load distributions appears to be an important problem in the application of power-spectral analysis to gust-load problems; therefore, some experimental gust-load distributions are examined for normality. Two applications of power-spectral

methods to the calculation of gust loads are also given in this section in order to obtain some insight into the relations between airplane characteristics and loads in continuous rough air. In the first series of calculations, the input-output relations are used to calculate the standard deviation of loads for a selected series of idealized responses to a step gust. The second series of calculations is made to determine the variations in the standard deviation of load for individual variations of certain geometric and aerodynamic parameters of an idealized transport airplane. The indicated variations in load intensity in this application are compared with those derived by conventional techniques of using the peak load response to an idealized discrete gust.

## Observed Distributions of Loads

In order to determine whether frequency distributions of load are actually normal distributions, recourse was made to some available experimental gust-load time-history data. Time-history records of the normal acceleration for two airplanes of the same type (differing only slightly in center-of-gravity position) in side-by-side flight through continuous rough air at low altitudes above generally flat terrain were available from a recent investigation. The test conditions and summaries of the data are presented in reference 10. The normal-acceleration time-history records for about a 2-minute section of one run at 450 miles per hour were evaluated in detail by taking readings at intervals of 1/20 second, roughly one reading for each 4 chords of airplane travel. The frequency distributions for the two airplanes are summarized in table I. (Additional data of the same type were also examined but do not appear to warrent reporting in detail at this time.) In determining these distributions, the 1 g level was assumed to be at the mean value of the disturbance. (This assumption is frequently used in gust evaluations in view of the difficulty in exactly determining the 1 g line for the flight condition.) The other primary characteristics of the observed frequency distribution, standard deviation $\sigma$, coefficient of skewness $\alpha_3$, and coefficient of kurtosis $\alpha_4$ are also given in table I where the statistical characteristics of the distribution were determined by the following relations:

$$\sigma = \left[\frac{\Sigma(\Delta n - \overline{\Delta n})^2}{N}\right]^{1/2} \qquad (30a)$$

$$\alpha_3 = \frac{1}{\sigma^3} \frac{\Sigma(\Delta n - \overline{\Delta n})^3}{N} \qquad (30b)$$

$$\alpha_4 = \frac{1}{\sigma^4} \frac{\Sigma(\Delta n - \overline{\Delta n})^4}{N} \qquad (30c)$$

where $N$ is the number of observations. For a normal distribution $\alpha_3 = 0$ and $\alpha_4 = 3$. The distributions of table I are shown as frequency polygons in figures 3(a) and 3(b). Also shown in the figures are the normal distributions fitted in accordance with standard statistical procedures by means of the calculated standard deviations of table I.

The fit of the normal distribution to the data for airplane A shows some tendency of the normal distribution to underestimate the concentration of values about the mean of the distribution while the fit of the data of airplane B appears generally good. In order to test the hypothesis that the observed samples are from a normal distribution, statistical procedures were applied to the observed statistical parameters. The results of these tests indicated that the distribution of $\Delta n$ for airplane B could be considered from a normal distribution, whereas the distribution for airplane A would not be assumed from a normal distribution. The magnitude of the departure from normality did not, however, appear large in this case.

In order to permit examination of the behavior of the distributions at the larger values of load factor which are of concern, the observed relative cumulative frequency distributions and the fitted cumulative probability distributions are shown in figure 4. The curves for both the probability of exceeding given values and the probability of being less than given values are shown on semilogarithmic paper in order to permit comparison at both the large positive and negative acceleration increments. Examination of these figures indicates that the data for airplane B are in excellent agreement with the fitted curves. For airplane A, the over-all agreement between observed data and fitted curve appears reasonable although some discrepancy between the observed distribution and the fitted curve is apparent particularly at the larger negative values of $\Delta n$. These discrepancies are in general, not large, however, and might, for example, be due to piloting-technique effects. However, the lack of consistency in the results indicates the need for further study of the question of the normality of the distribution of load.

In order to examine the question of normality somewhat further at this time, recourse was made to additional data on frequency distributions of load increment under conditions similar to those represented in figures 3 and 4. Examination of these additional data indicates that although the distributions were generally close to normal, in a number of cases, more large accelerations were experienced than expected for a normal distribution. Consideration of the time-history records from which these distributions were obtained indicated that these departures from normality were associated with lack of homogeneity in the turbulence intensity during the flight run. Only for short runs of constant level turbulence did the distributions appear normal.

The manner in which the departures from normality arise in nonhomogeneous turbulence may be clarified by an example. Consider a flight run through rough air consisting of somewhat more severe turbulent conditions during the second part of the run. The over-all distribution of loads may for this condition be expected to consist of two normal distributions, one for each part of the run. The two normal distributions would be expected to have mean values of zero for the load factor increment but different standard deviations. The combined distribution for the whole run can be shown (appendix) to depart from normality with an excess of observations at the center and at the larger values of load increment. This mechanism can account for the departures from normality observed in the data examined.

In view of the foregoing indications, it would appear reasonable for the present to assume that for locally homogeneous turbulence of the type represented in figures 3 and 4 the frequency distribution of load increments may be expected to approximate a normal distribution. The approximate normality of the load distribution for homogeneous turbulence permits the use of the relations derived earlier between the frequency distribution of loads and the power spectrums and permits the representation of the load intensity by a single number, the standard deviation of the frequency distribution of load. This unification of the power-spectral-density function and the probability distribution of loads even for limited conditions is of considerable importance since in many load studies the relative loads in continuous rough air of two airplanes (or one airplane at two flight conditions) are of interest. For this case the use of the standard deviation as derived from the power-spectral analysis appears to provide a direct measure of the relative loads.

In view of the foregoing indications that a lack of turbulence homogeneity can cause significant departures from a normal distribution of loads, further studies of the distribution of loads under various atmospheric conditions are needed. It may be expected that the turbulence connected with such dynamic phenomena as thunderstorms which have a large-scale physical structure and short life cycle may not be stationary

random. For these conditions, the airplane load histories might have distributions that depart significantly from normality. This limitation may not, however, be too serious since even in these cases the standard deviation of loads may still provide a measure of load intensity although one not as simply interpretable in terms of the probability distribution as in the case of the normal distribution.

## Relation of Step Response Characteristics to Loads in Continuous Rough Air

Examination of calculated responses to entry of a sharp-edge gust for airplanes representative of conventional transport types has indicated that the shape of the response curve up to the peak acceleration depends primarily on the gust penetration function (Küssner function). After the peak value which occurs close to 6 chords of gust penetration, the character of the response appears to be primarily a function of airplane stability and to approximate the short-period oscillation of the airplane. On the basis of these properties, a limited series of response curves to a sharp-edge gust were selected to represent variations in airplane dynamic longitudinal stability. The incremental acceleration responses in g's to a 1-foot-per-second sharp-edge gust were assumed to be given by the following expressions:

$$\left.\begin{aligned} \Delta n(s) &= \frac{1}{30}\sin\frac{\pi}{12}s && (0 \leq s \leq 6) \\ \Delta n(s) &= \frac{1}{30}e^{-b(s-6)}\cos k_o(s-6) && (6 \leq s \leq \infty) \end{aligned}\right\} \quad (31)$$

Equations (31) represent a quarter sine wave up to a fixed peak value of 0.033g at 6 chords and a damped oscillatory function for the remaining portion of the response. The parameters $b$ and $k_o$ can be considered to represent the damping and frequency parameters, respectively, of the response following the peak load. In figure 5, plots of equations (31) are shown for nine selected cases covering three values for each of the two parameters. The values were selected to sample a wide range of airplane response characteristics and represent variations in wave length from 40 to 150 chords and variations in damping from light to almost critical damping.

In view of the linearity of the systems being considered, the multiplication of the response $\Delta n(s)$ of equations (31) by a constant results in the multiplication of the frequency-response function and the standard deviation of the output in turn by the same constant. Thus, the effect on the standard deviation of load of variations in the peak values of $\Delta n$ for given values of $k_o$ and $b$ is apparent and the consideration of an amplitude factor in equations (31) does not warrant more detailed discussion.

The frequency response function $\tilde{T}(i\nu)$ was determined analytically from the sharp-edge-gust response given by equations (31) by using equations (21). The amplitude squared of the transfer function $\left|\tilde{T}(i\nu)\right|^2$ is given by

$$\left|\tilde{T}(i\nu)\right|^2 = \frac{1}{(30)^2}\left\{\frac{\nu}{2}\left[\frac{\sin 6\left(\frac{\pi}{12}-\nu\right)}{\frac{\pi}{12}-\nu} - \frac{\sin 6\left(\frac{\pi}{12}+\nu\right)}{\frac{\pi}{12}+\nu}\right] + \frac{\left(b^2+k_o^2+\nu^2\right)b\nu \sin 6\nu + \left(b^2-k_o^2+\nu^2\right)\nu^2\cos 6\nu}{\left(b^2+k_o^2-\nu^2\right)^2+4\nu^2b^2}\right\}^2 +$$

$$\frac{1}{(30)^2}\left\{\frac{\left(b^2+k_o^2+\nu^2\right)b\nu\cos 6\nu - \left(b^2-k_o^2+\nu^2\right)\nu^2\sin 6\nu}{\left(b^2+k_o^2-\nu^2\right)^2+4\nu^2b^2} - \frac{\nu}{2}\left[\frac{\cos 6\left(\frac{\pi}{12}-\nu\right)-1}{\frac{\pi}{12}-\nu} + \frac{\cos 6\left(\frac{\pi}{12}+\nu\right)-1}{\frac{\pi}{12}+\nu}\right]\right\}^2 \qquad (32)$$

Plots of equation (32) are shown in figure 6 for the nine cases considered in figure 5.

The reduced power-spectral-density function of atmospheric turbulence, shown in figure 2, was used as the input. For any particular weather condition, the power-spectral-density function would have to be adjusted by taking into account the actual average power of the input. This change would, however, only involve an appropriate linear change in the ordinate scale and would not affect the relative indications of the present comparisons.

Examination of figure 6 indicates that, as the damping of the oscillation is decreased (b decreased), the amplitude increases rapidly in the neighborhood of the oscillation frequency $k_o$. The frequency response function remains relatively unchanged over the rest of the frequency range. On the other hand, variations in the oscillation frequency $k_o$, for fixed values of b, have a minor effect on the shape of the function but the peak values change (note changes in the ordinate scale) and occur at values of $\nu$ close to $k_o$.

The power-spectral-density function of the acceleration-increment output was obtained from equations (18) and (22) by the relation

$$\hat{\Phi}_o(\Omega) = \hat{\Phi}_i(\Omega)\left|\tilde{T}(ic\Omega)\right|^2 \tag{33}$$

For convenience, an airplane chord of 9.67 feet, the same value as the chord of the airplane used to obtain the input spectrum, was assumed for this series of calculations. The power-spectral densities of the acceleration-increment output $\hat{\Phi}_o(\Omega)$ for the conditions being considered are shown in figure 7. Since the power-spectral-density function of atmospheric turbulence was not known for frequencies $\Omega$ less than 0.0016 radian per foot, the output spectrum could not be determined in this region. The output spectrums were, however, extrapolated to zero at $\Omega = 0$ in order to complete the output spectrum at the low frequencies. The extrapolations are indicated in figure 7.

Examination of figure 7 indicates that as damping is decreased the output spectrums for each value of $k_o$ increase rapidly in the neighborhood of the oscillatory frequency $\Omega = \frac{k_o}{c} = \frac{k_o}{9.67}$. For given values of damping, however, the power spectrums do not vary appreciably in shape but the peak values shift in frequency with $k_o$. Thus, the total power of the spectrum as measured by the integral of the spectral function appears to be largely independent of $k_o$ and primarily a function of b for the conditions investigated. This result can be seen from figures 6 and 7 to be a consequence of both the variations in response functions and the rapid decrease of power of the gust spectrum with increasing frequency.

The rapid increase of the loads with decreased damping is more clearly illustrated in figure 8, which shows the standard deviation of loads $\sigma$ (the square root of the integral of the power spectrum) as a function of frequency for the several values of $b$ considered. The standard deviations of the acceleration increment $\sigma$ were obtained from the output spectrums by using equation (29). In the evaluation of equation (29), the output spectrums as extrapolated from a frequency of 0.0016 radian per foot to C (fig. 7) was used and the area of the output spectrums for values of $\Omega$ greater than 0.028 was assumed negligible. The figure indicates clearly that the load level, as measured by the standard deviation, is largely independent of the frequency parameter $k_o$ but varies appreciably when the damping parameter $b$ is changed, the variation of the standard deviation being of the order of two to one for the conditions considered.

The results imply that the short-period response characteristics and particularly the damping characteristics have an appreciable effect on the airplane loads in continuous rough air. In contrast, the airplane peak-load response to discrete gusts can be shown for the present example to be affected only to a minor extent by the short-period damping characteristics. In view of these differences between the indications of power-spectral and discrete-gust calculations, discrete-gust calculations may not adequately reflect differences in the gust loads in continuous rough air between airplanes differing in dynamic stability characteristics. In particular these results indicate that discrete-gust calculations may not be adequate for the determination of loads in continuous rough air for modern high-speed airplanes which in contrast to the airplanes of the past have relatively poor short-period damping. More complete accounting of airplane short-period characteristics in gust-load analysis would appear to be required in these cases.

The variations of the response to a step gust assumed in the present illustration represent idealized conditions in which the characteristics of the airplane response to a step gust were changed in a simple manner. In practice, the change of almost any airplane parameter will modify the response to a step gust in a complex manner. Thus, a change of an airplane parameter will affect the peak-load value, the location of peak, and both the frequency and damping of the subsequent oscillation. Consequently, the problem of optimum design for gust-load reduction is extremely complicated and beyond the scope of the present study. The effects of variations in airplane geometry on gust loads are, to some extent, indicated in the second illustration in which the complete changes in the response to a step gust for limited variations in each of selected parameters of an idealized airplane are considered.

## Effect on Loads of Some Variations in Airplane Geometric and Aerodynamic Parameters

In order to obtain an indication of the relation between some airplane geometric and aerodynamic parameters and loads in continuous rough air, the power-spectral-density functions of load based on the turbulence spectrum of figure 2 were calculated for selected variations in airplane characteristics. An idealized transport airplane was used as a basic configuration. Characteristics of this basic configuration are listed in table II. In addition, values of each of 11 airplane parameters listed were varied separately in order to obtain an "increased" condition and a "decreased" condition, as indicated in the table. (In the case of the center-of-gravity position, the increased condition represents the forward center-of-gravity position.) The 23 conditions covered in these calculations represented stable airplanes with static margins varying from $-0.25\bar{c}$ to $-0.50\bar{c}$ where $\bar{c}$ is mean aerodynamic chord.

The responses to a unit step gust with a velocity of 1 foot per second $A(x)$ for the two-degrees-of-freedom case, vertical motion and pitch, were available for the 23 cases of table II from an unpublished study based on the methods of reference 6. The frequency-response functions were determined by means of equations (17). The power-spectral-density function for acceleration output corresponding to the turbulence input of figure 2 was obtained for each condition by use of equation (18). The standard deviation of acceleration increment was determined for each case from equation (29) by the relation

$$\sigma = \left[\int_0^\infty \hat{\Phi}_o(\Omega)\, d\Omega\right]^{1/2}$$

In performing this integration, it was assumed that the output for frequencies of $\Omega$ greater than 0.028 was negligible. The output spectrums were also faired to a value of zero at $\Omega$ equal to zero as in the previous application.

As a basis for comparing the results of the indications of the spectral analysis with the indications of conventional types of analysis based on responses to single representative gusts, a triangular gust with a gradient distance (distance from zero to peak value) of 10 chords was selected as a representative gust condition. This gust condition represents an average gradient distance for the more severe gust loads and is frequently used for analysis purposes as a measure of the airplane loads in rough air. The peak load-factor value $\Delta n_{max}$ for a 1-foot-per-second triangular gust having a gradient distance of 10 chords was calculated for the two-degrees-of-freedom case for each of the 23 conditions considered.

The results of the power-spectral and single-gust calculations are compared in figure 9 for each of the 23 conditions. The abscissa in the figure represents the single-gust peak response, the ordinate the power-spectral-density measure of load intensity. For ease in comparing the relative changes, both single-gust and spectral-calculation results are shown in terms of the basic airplane response. Thus, the abscissa is given as $\Delta n_{max}/(\Delta n_{max})_{basic}$ and the ordinate, as $\sigma/\sigma_{basic}$. The line of equality $\frac{\Delta n_{max}}{(\Delta n_{max})_{basic}} = \frac{\sigma}{\sigma_{basic}}$ is shown as a reference. If both methods of analysis gave the same percentage change in load for a given change from the basic airplane, the plotted point would fall on the line of equality.

Examination of the results shown in figure 9 indicates that to a first approximation both the standard deviation of loads and the maximum load for a 10-chord-gradient triangular gust show the same trends for variations of the airplane parameters considered. The largest changes in load level are associated with changes in airplane weight, wing area, air density, and slope of the wing lift curve as might be expected from the sharp-edge-gust relation. Inspection of the figure indicates that complex second-order differences that may be important exist in the indications given by the two measures of loads. As an example, for the variations of loads for changes of wing area the figure indicates that for the 20-percent increase in wing area (represented by the square), the value of $\Delta n_{max}/(\Delta n_{max})_{basic}$ increases about 18 percent. The relative standard deviation $\sigma/\sigma_{basic}$, however, increases only about 7 percent. This difference appears to be a consequence of the greater sensitivity of the power-spectral analysis to the changes in airplane stability introduced by the increased wing area; the increase in wing area results in a small decrease in the frequency of the response to a step gust but a more pronounced increase in the damping. The present results also suggest similar differences between the two analyses for changes in airplane weight and slope of the wing lift curve.

The variations considered for the remaining parameters such as tail length, tail area, and tail slope of the lift curve, in general, yield minor variations in loads. The variations in $\Delta n_{max}/(\Delta n_{max})_{basic}$ for these cases are however less than $\pm 2$ percent while the variations for the standard deviations are generally somewhat larger, $\pm 4$ percent. In figure 9 the 12-percent-chord rearward movement of the center-of-gravity position $l_w$ yields about a 3-percent increase in $\Delta n_{max}/(\Delta n_{max})_{basic}$ but a 9 percent increase in the relative standard deviation. In this case, the larger increase in the standard deviation appears largely associated with the movement of the peak of the frequency response function to lower frequency and thus larger gust spectral power.

For the stable airplane configurations considered, the power-spectral analysis and the single-gust peak-load response yield trends for changes in parameter values that are generally consistent. Differences that may be important are, however, discernible and appear associated with the greater dependence of the standard deviation of loads on the dynamic stability characteristics of the airplane. It would be expected from the first application that for larger variations in the damping characteristics of the short-period oscillation, the differences between the two types of analysis would be appreciably larger than obtained in the present illustration.

## SUMMARY OF RESULTS

The analysis of the application of power-spectral methods of analysis to gust-load problems has indicated the following results:

1. The application of power-spectral methods of analysis to load calculations provides a measure of load intensity for continuous rough air in terms of the standard deviation (root mean square) of the load output.

2. The probability distribution of load intensity in homogeneous rough air appears to approximate a normal distribution.

3. For the case of the normally distributed output, the standard deviation of load completely describes the probability distribution of loads specifying the proportion of total time that various load values are exceeded.

4. The application of power-spectral relations to a selected series of systematic variations in the frequency and damping characteristics of the airplane load response to a step-gust input indicates that the damping characteristics of the indicial response are the primary characteristics in determining the loads in continuous rough air. This result appears of significance in regard to high-speed airplanes and missiles where the short-period longitudinal damping may be poor.

5. Calculations for a limited series of conventional and stable airplane configurations indicates that the loads in continuous rough air for variations in individual airplane geometric and aerodynamic parameters are to a first approximation adequately reflected by the peak-load response to the arbitrary 10-chord triangular gust commonly used. However, differences are discernible between the indications of the continuous-gust and discrete-gust calculations and appear largely associated with differences in the effects of stability changes on the loads for the two gust conditions.

## SUGGESTIONS FOR FUTURE RESEARCH

The foregoing results appear to indicate that power-spectral methods are well-suited to the calculation of loads in continuous rough air. A number of problems exist and require further investigation. These include

(1) The determination of the power-spectral-density functions of atmospheric turbulence for a wide range of atmospheric conditions.

(2) The determination of the conditions under which normal distributions of the load time history apply.

(3) The investigation of the effects of the nonuniformity of gusts across the airplane span on the application of these techniques.

(4) The experimental verification of theoretical determinations of airplane indicial responses over the range required to determine usable frequency-response functions.

(5) The investigation of the relations between the power spectrums and the frequency distribution of load-increment peaks and other quantities of interest in structural design.

Langley Aeronautical Laboratory,
National Advisory Committee for Aeronautics,
Langley Field, Va., September 29, 1952.

# APPENDIX

## DISTRIBUTION OF GUST LOADS IN NONHOMOGENEOUS ROUGH AIR

If the two normal frequency distributions of load increment with zero mean are defined by

$$\left.\begin{aligned} N_1 f_1(\Delta n) &= \frac{N_1}{\sigma_1\sqrt{2\pi}} e^{-\frac{1}{2}\left(\frac{\Delta n}{\sigma_1}\right)^2} \\ N_2 f_2(\Delta n) &= \frac{N_2}{\sigma_2\sqrt{2\pi}} e^{-\frac{1}{2}\left(\frac{\Delta n}{\sigma_2}\right)^2} \end{aligned}\right\} \quad \text{(A1)}$$

where

$f_1(\Delta n), f_2(\Delta n)$ respective probability density functions

$N_1, N_2$ respective number of observations for each distribution

$\sigma_1, \sigma_2$ standard deviations of respective distributions

the combined distribution is defined by

$$Nf(\Delta n) = N_1 f_1(\Delta n) + N_2 f_2(\Delta n) \quad \text{(A2)}$$

where $N = N_1 + N_2$. This distribution is examined for normality.

Since the two frequency distributions $N_1 f_1(\Delta n)$ and $N_2 f_2(\Delta n)$ are each normal with mean zero, the combined distribution $Nf(\Delta n)$ is also symmetrical about zero. Consequently, for the moments of the frequency distribution $\mu_m$ defined by

$$\mu_m = \int_{-\infty}^{\infty} (\Delta n)^m f(\Delta n)\ d(\Delta n) \tag{A3}$$

where $m$ is a positive number and designates the moment order, the following relations apply

$$\left.\begin{aligned} \mu_m &= 0 \qquad (m \text{ odd}) \\ \mu_m &\neq 0 \qquad (m \text{ even}) \end{aligned}\right\} \tag{A4}$$

For a normal distribution, the coefficient of kurtosis $\alpha_4$ defined by

$$\alpha_4 = \frac{\mu_4}{\mu_2^2} = \frac{\mu_4}{\sigma^4} \tag{A5}$$

has a fixed value

$$\alpha_4 = 3 \tag{A6}$$

In order to examine the normality of the distribution defined by equation (A2), consider only the value of $\alpha_4$, the coefficient of kurtosis, for that frequency distribution.

By definition, the coefficient of kurtosis $\alpha_4$ for the distribution of equation (A2) is given by

$$\alpha_4 = \frac{\frac{1}{N_1 + N_2}\left[\int_{-\infty}^{\infty} (\Delta n)^4 N_1 f_1\ d(\Delta n) + \int_{-\infty}^{\infty} (\Delta n)^4 N_2 f_2(\Delta n)\ d(\Delta n)\right]}{\left\{\frac{\int_{-\infty}^{\infty} (\Delta n)^2 \left[N_1 f_1(\Delta n) + N_2 f_2(\Delta n)\right]\ d(\Delta n)}{N_1 + N_2}\right\}^2} \tag{A7}$$

which when simplified yields

$$\alpha_4 = \frac{\frac{3}{N_1 + N_2}\left(N_1\sigma_1^4 + N_2\sigma_2^4\right)}{\left(\frac{N_1\sigma_1^2 + \mu_2\sigma_2^2}{N_1 + N_2}\right)^2} \tag{A8}$$

From equation (A6), a necessary condition for the distribution $Nf(\Delta n)$ to be normal is that $\alpha_4$ be equal to 3. From equation (A8) this condition is obviously true only when

$$N_1\sigma_1^4 + N_2\sigma_2^4 = \frac{1}{N_1 + N_2}\left(N_1\sigma_1^2 + N_2\sigma_2^2\right)^2 \tag{A9}$$

Expanding the term on the right and simplifying yields

$$\sigma_1^4 + \sigma_2^4 = 2\sigma_1^2\sigma_2^2 \tag{A10}$$

Equation (A10) is thus a necessary condition for the distribution defined by (A2) to be normal. However, from the inequality

$$a^2 + b^2 > 2ab \qquad (a \neq b) \tag{A11}$$

the only condition for which equation (A10) holds is when $\sigma_1 = \sigma_2$. Thus the distribution $f(\Delta n)$ has a normal distribution only for the trivial case $\sigma_1 = \sigma_2$. If $\sigma_1 \neq \sigma_2$, it also follows from equation (A10) that the coefficient of kurtosis $\alpha_4$ for $Nf(\Delta n)$ given by equation (A8) is greater than 3. The combined distribution consequently has an excess of kurtosis. Before considering the significance of the excess kurtosis, it is well to note that the present derivation was restricted to the combination of two distributions for simplicity. It is simple although tedious to verify that similar results are obtained for the combination of three or more distributions.

The significance of the excess kurtosis for the combined distribution may perhaps be best indicated with a sketch. The sketch shows two symmetrical relative frequency distributions having the same standard deviations, one a normal distribution $(\alpha_4 = 3)$ the other a nonnormal distribution with $\alpha_4 > 3$. The nonnormal distribution is derived from the normal by a shift of mass outward from the central portion of the distribution and also a shift of mass inward to maintain the same standard deviation for the two cases. Thus, it is apparent that the predominent feature of the distribution having excess kurtosis is a greater concentration of mass at the center and at the outboard regions of the distribution than for the normal-distribution case.

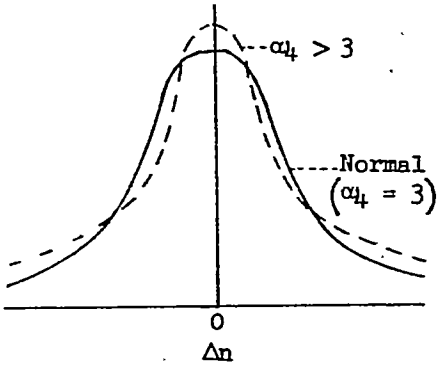

## REFERENCES

1. Donely, Philip: Summary of Information Relating to Gust Loads on Airplanes. NACA Rep. 997, 1950. (Supersedes NACA TN 1976.)

2. Clementson, Gerhardt C.: An Investigation of the Power Spectral Density of Atmospheric Turbulence. Ph. D. Thesis, M.I.T., 1950.

3. Wiener, Norbert: Generalized Harmonic Analysis. Acta Mathematica, vol. 55, 1930, pp. 117-258.

4. James, Hubert M., Nichols, Nathaniel B., and Phillips, Ralph S.: Theory of Servomechanisms. McGraw-Hill Book Co., Inc., 1947.

5. Liepmann, H. W.: An Approach to the Buffeting Problem From Turbulence Considerations. Rep. No. SM-13940, Douglas Aircraft Co., Inc., Mar. 13, 1951.

6. Mazelsky, Bernard, and Diederich, Franklin W.: A Method of Determining The Effect of Airplane Stability on the Gust Load Factor. NACA TN 2035, 1950.

7. Chippendale, George R., and Clement, Warren F.: A Statistical Study of Atmospheric Turbulence by Flight Measurements. Rep. No. T-2, M.S. Thesis, M.I.T., 1951.

8. Rice, S. O.: Mathematical Analysis of Random Noise. Pts. I and II. Bell Syst. Tech. Jour., vol. XXIII, no. 3, July 1944, pp. 282-332; Pts. III and IV, vol. XXIV, no. 1, Jan. 1945, pp. 46-156.

9. Cramér, Harald: Mathematical Methods of Statistics. Princeton Univ. Press, 1946.

10. Binckley, E. T., and Funk, Jack: A Flight Investigation of the Effects of Compressibility on Applied Gust Loads. NACA TN 1937, 1949.

TABLE I.- FREQUENCY DISTRIBUTIONS OF ACCELERATION INCREMENT

| Airplane A | | Airplane B | |
|---|---|---|---|
| Acceleration increment, $\Delta n$, g units | Number | Acceleration increment, $\Delta n$, g units | Number |
| -0.777 to -0.727 | 2 | -0.719 to -0.669 | 1 |
| -.727 to -.677 | 0 | -.669 to -.619 | 1 |
| -.677 to -.627 | 1 | -.619 to -.569 | 2 |
| -.627 to -.577 | 0 | -.569 to -.519 | 4 |
| -.577 to -.527 | 2 | -.519 to -.469 | 11 |
| -.527 to -.477 | 2 | -.469 to -.419 | 12 |
| -.477 to -.427 | 7 | -.419 to -.369 | 22 |
| -.427 to -.377 | 11 | -.369 to -.319 | 35 |
| -.377 to -.327 | 16 | -.319 to -.269 | 60 |
| -.327 to -.277 | 33 | -.269 to -.219 | 99 |
| -.277 to -.227 | 67 | -.219 to -.169 | 119 |
| -.227 to -.177 | 104 | -.169 to -.119 | 200 |
| -.177 to -.127 | 157 | -.119 to -.069 | 245 |
| -.127 to -.077 | 241 | -.069 to -.019 | 254 |
| -.077 to -.027 | 315 | -.019 to .031 | 266 |
| -.027 to .023 | 386 | .031 to .081 | 277 |
| .023 to .073 | 338 | .081 to .131 | 215 |
| .073 to .123 | 240 | .131 to .181 | 172 |
| .123 to .173 | 140 | .181 to .231 | 126 |
| .173 to .223 | 125 | .231 to .281 | 77 |
| .223 to .273 | 65 | .281 to .331 | 56 |
| .273 to .323 | 43 | .331 to .381 | 36 |
| .323 to .373 | 16 | .381 to .431 | 22 |
| .373 to .423 | 10 | .431 to .481 | 16 |
| .423 to .473 | 9 | .481 to .531 | 9 |
| .473 to .523 | 7 | .531 to .581 | 2 |
| .523 to .573 | 1 | .581 to .631 | 2 |
| .573 to .623 | 1 | | |
| Total | 2339 | Total | 2341 |
| $\overline{\Delta n}$ | 0 | $\overline{\Delta n}$ | 0 |
| $\sigma$ | 0.1505 | $\sigma$ | 0.1803 |
| $\alpha_3$ | -0.049 | $\alpha_3$ | -0.013 |
| $\alpha_4$ | 4.243 | $\alpha_4$ | 3.360 |

NACA

TABLE II.- VALUES OF AIRPLANE PARAMETERS

[U = 1 ft/sec; V = 308 ft/sec; $c_t$ = 7.58 ft]

| Airplane parameter | Basic | Increased (a) | Decreased (a) |
|---|---|---|---|
| $a_w$, per radian . . . . | 5.56 | 6.40 | 4.73 |
| $a_t$, per radian . . . . | 3.21 | 3.69 | 2.73 |
| S, sq ft . . . . . | 738 | 885 | 590 |
| $S_t$, sq ft . . . . . | 275 | 330 | 220 |
| $\rho$, slugs/cu ft . . . . | 0.002049 | 0.002378 | 0.001756 |
| $d\epsilon/d\alpha$ . . . . . | 0.5 | 0.6 | 0.4 |
| $l_w$, ft . . . . . | 0 | -1.26 | [b]1.26 |
| $l_t$, ft . . . . . | 35.38 | 39.26 | 31.54 |
| I, slug-ft$^2$ . . . . | 209,600 | 272,000 | 146,100 |
| c, ft . . . . . | 10 | 11.5 | 8.5 |
| W, lb . . . . . | 38,000 | 47,500 | 28,500 |

[a]Values indicate parameter changed for given condition whereas other parameters remain same as basic condition.

[b]Center of gravity rearward.

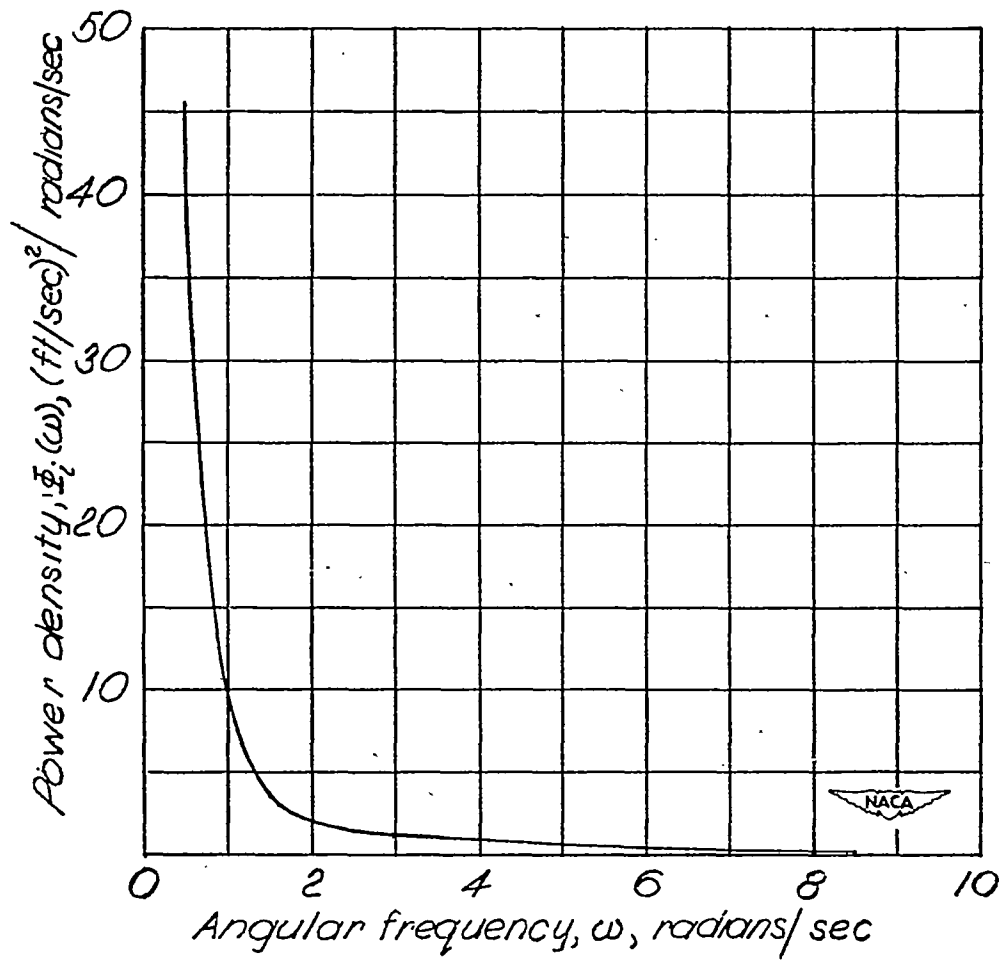


Figure 1.- Normalized power-spectral-density function for atmospheric vertical gust velocity $\Phi_1(\omega)$ for airspeed of 300 feet per second.

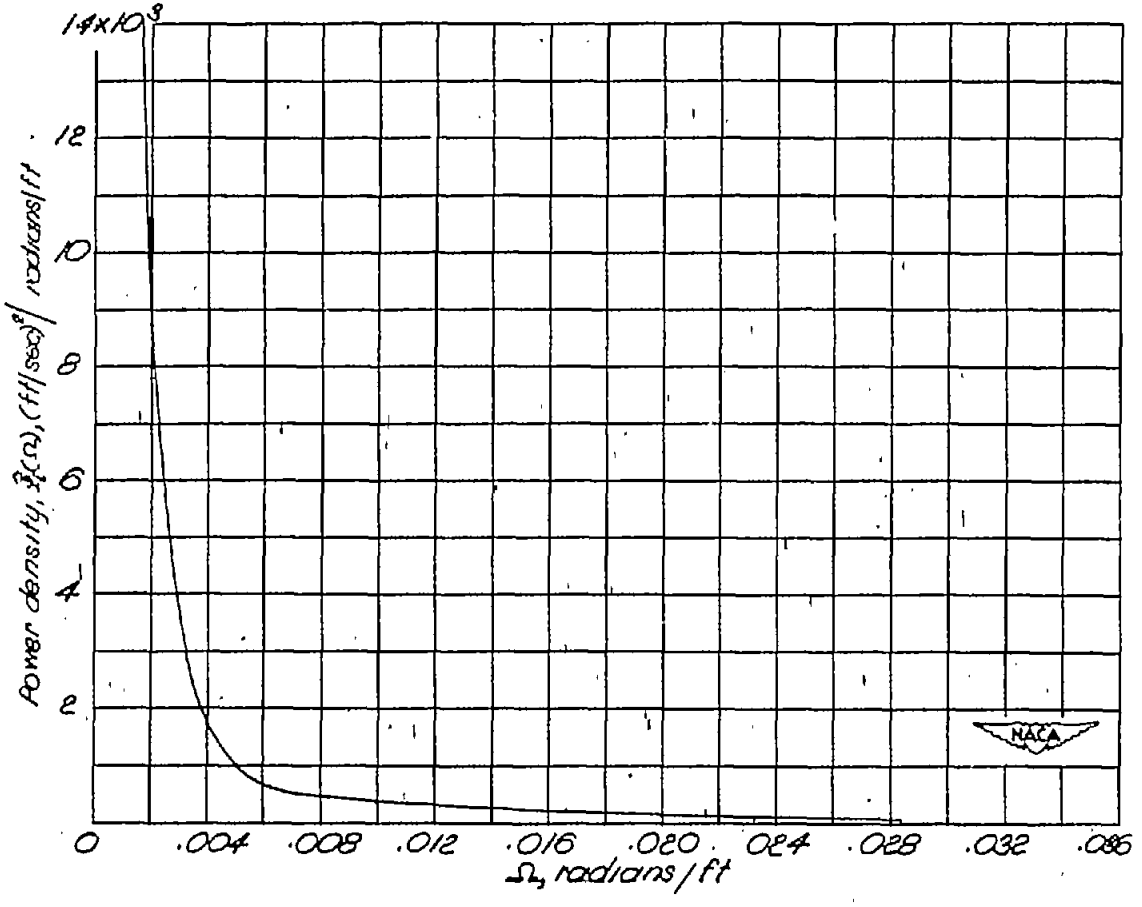


Figure 2.- Normalized power-spectral-density function for atmospheric vertical gust velocity $\hat{\Phi}_i(\Omega)$.

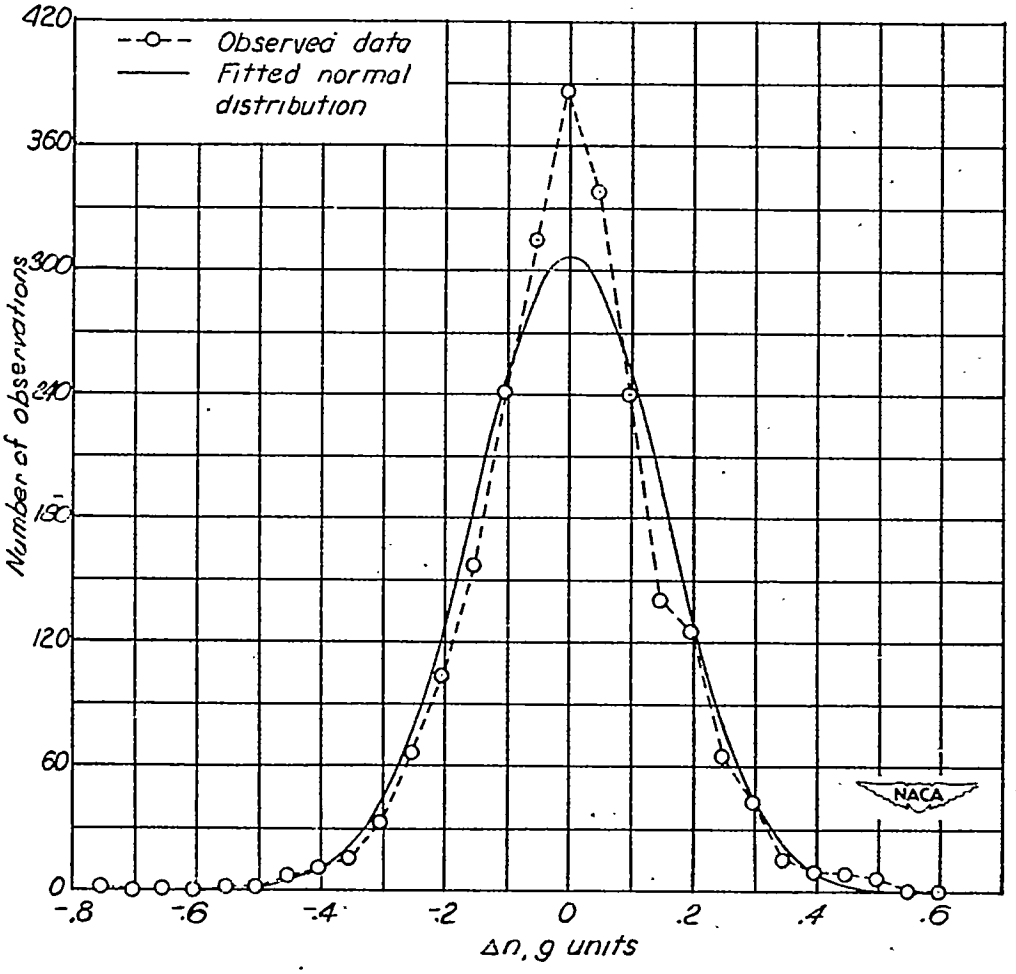


(a) Airplane A.

Figure 3.- Comparison of observed frequency distribution and fitted normal frequency distribution.

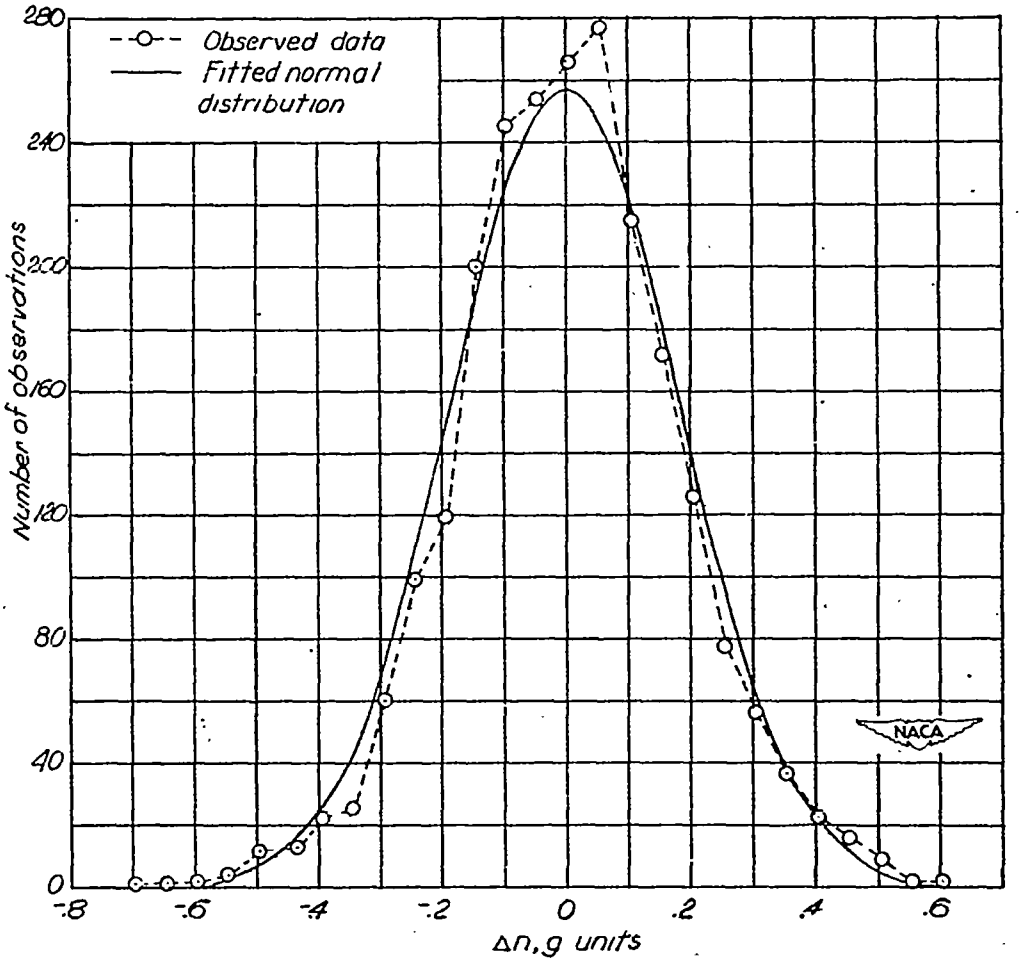


(b) Airplane B.

Figure 3.- Concluded.

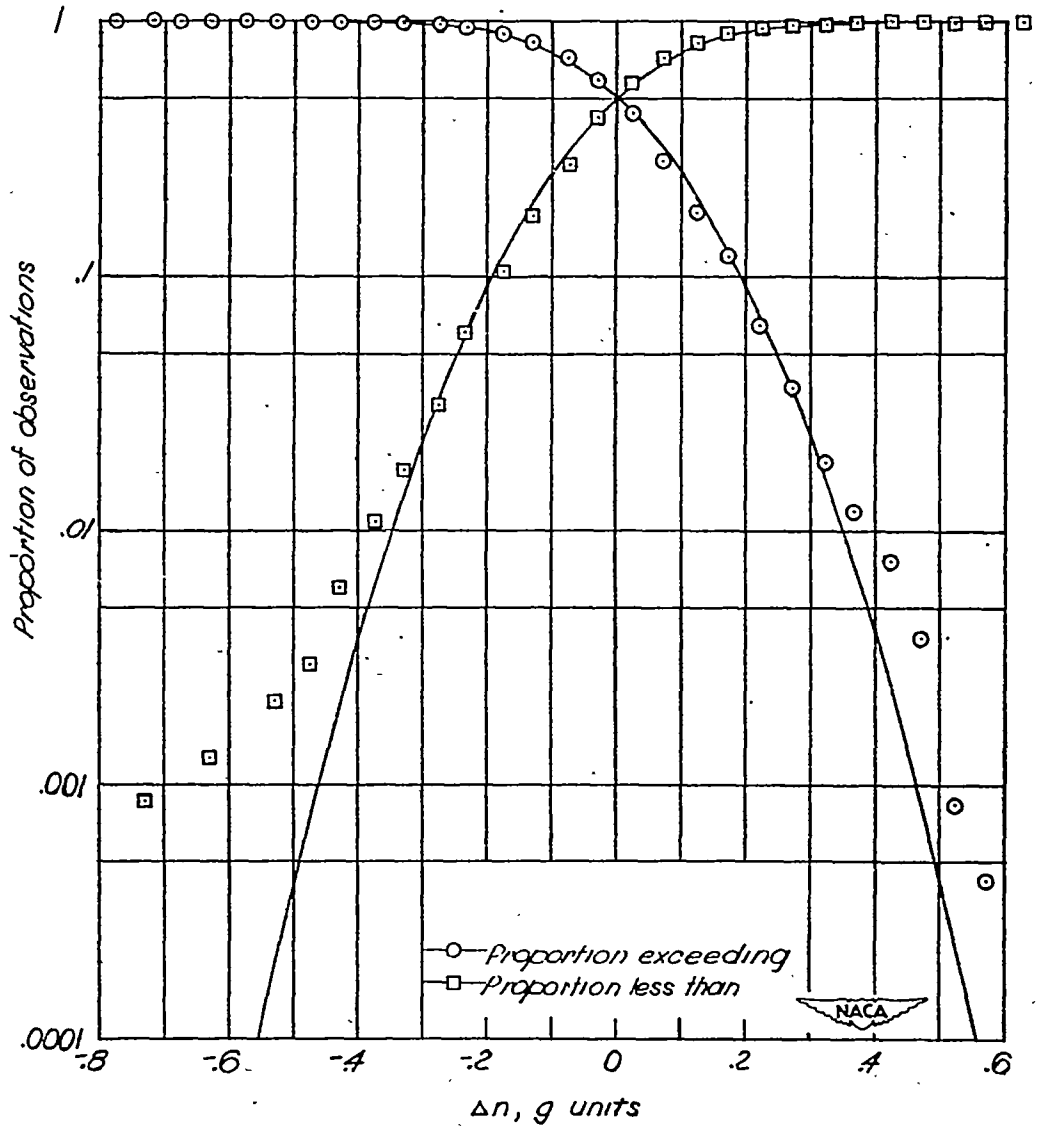


(a) Airplane A.

Figure 4.- Comparison of observed relative cumulative frequency distribution with fitted normal probability distribution.

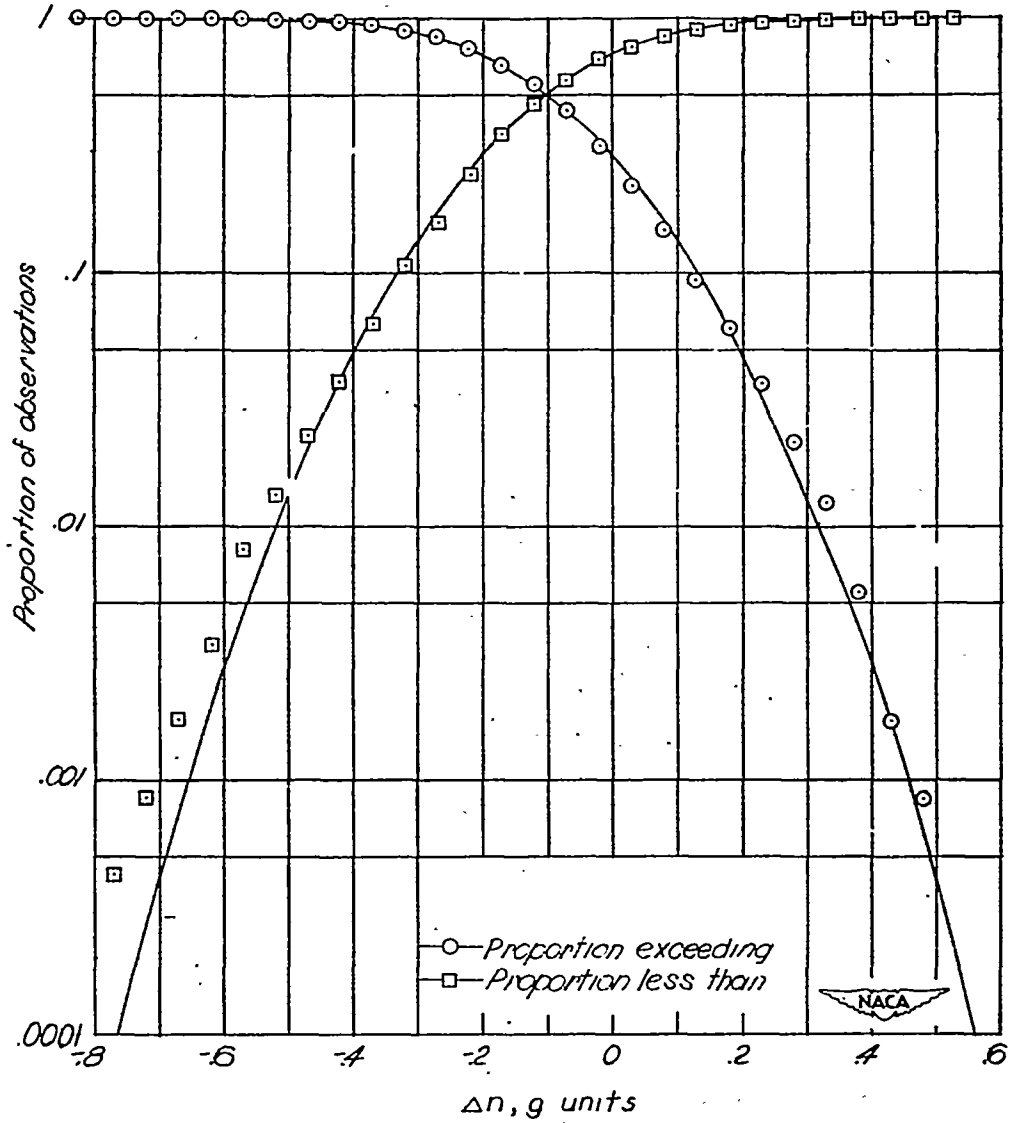


(b) Airplane B.

Figure 4.- Concluded.

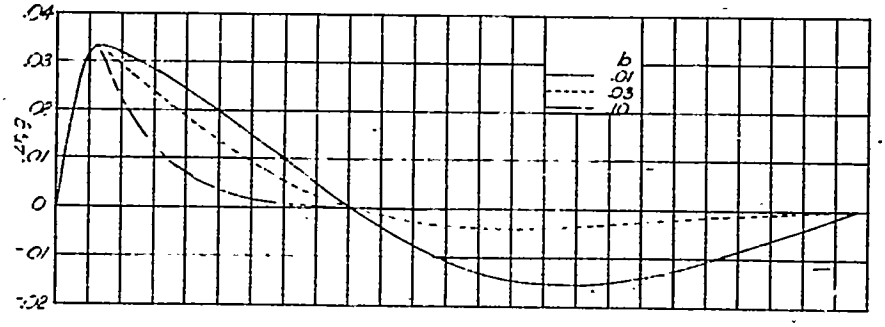


(a) $k_o = 0.04$.

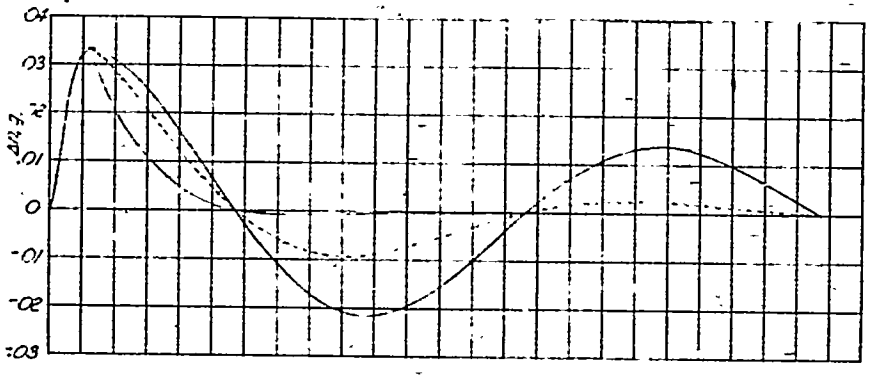


(b) $k_o = 0.07$.

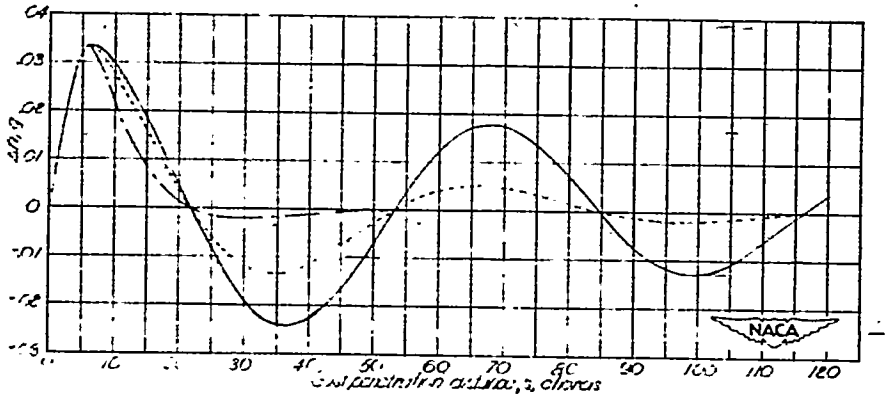


(c) $k_o = 0.10$.

Figure 5.- Load-factor-increment responses due to penetration of a sharp-edge gust for several stability conditions.

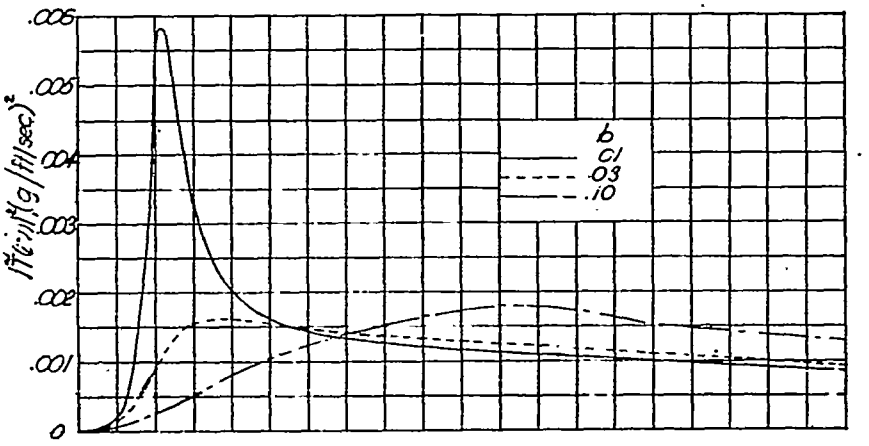


(a) $k_o = 0.04$.

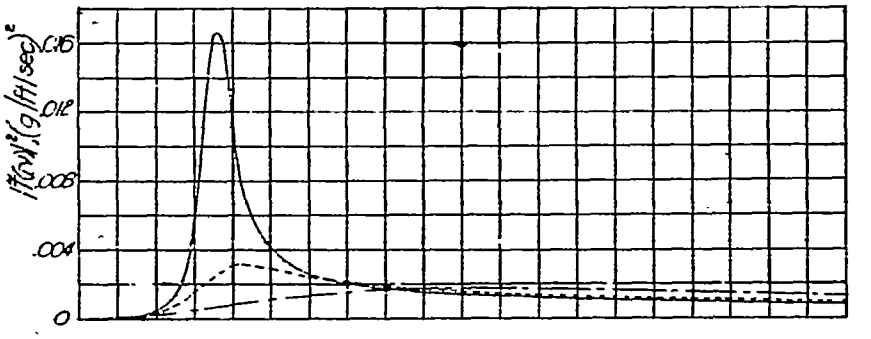


(b) $k_o = 0.07$.

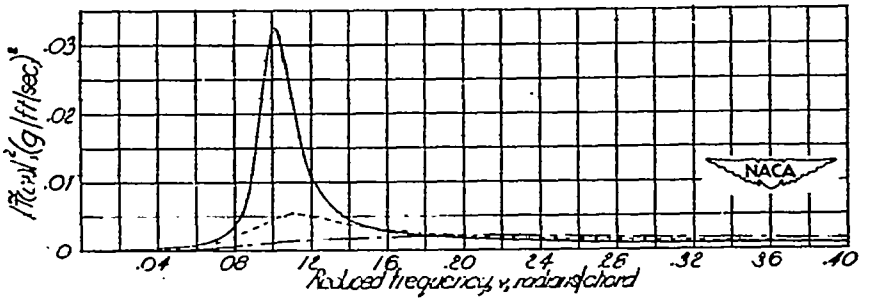


(c) $k_o = 0.10$.

Figure 6.- Modulus squared of transfer functions for selected variations of the frequency parameter $k_o$ and the damping parameter b.

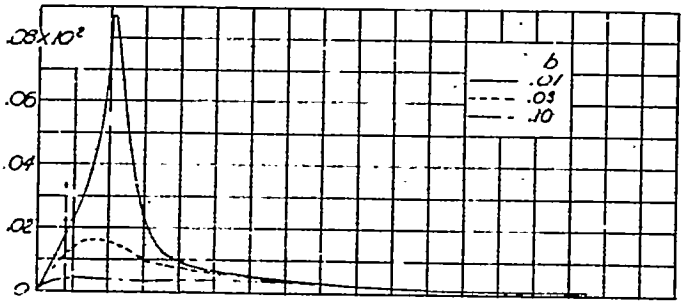


(a) $k_o = 0.04$.

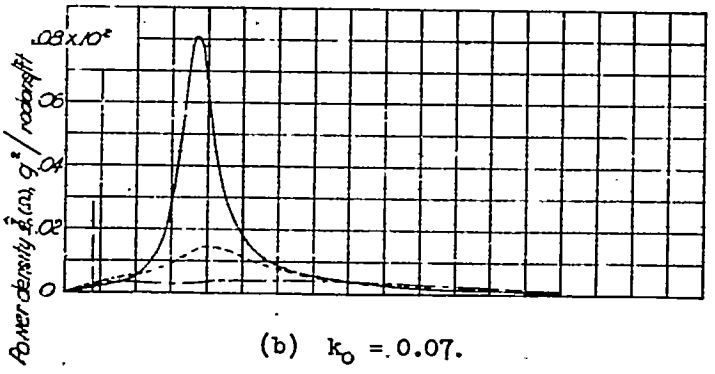


(b) $k_o = 0.07$.

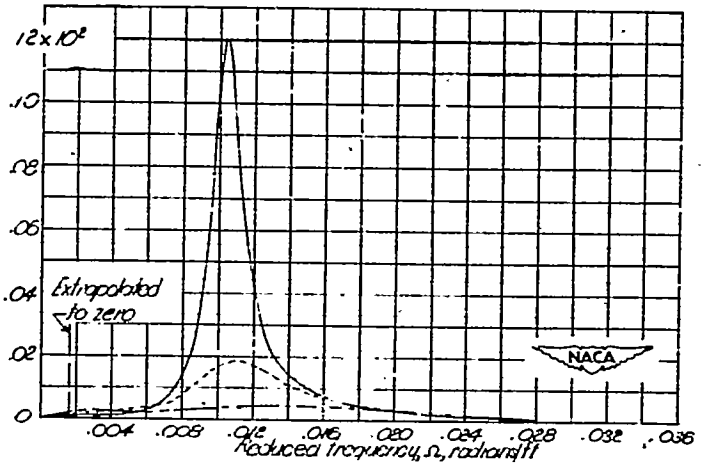


(c) $k_o = 0.10$.

Figure 7.- Power-spectral-density function of load-factor output.

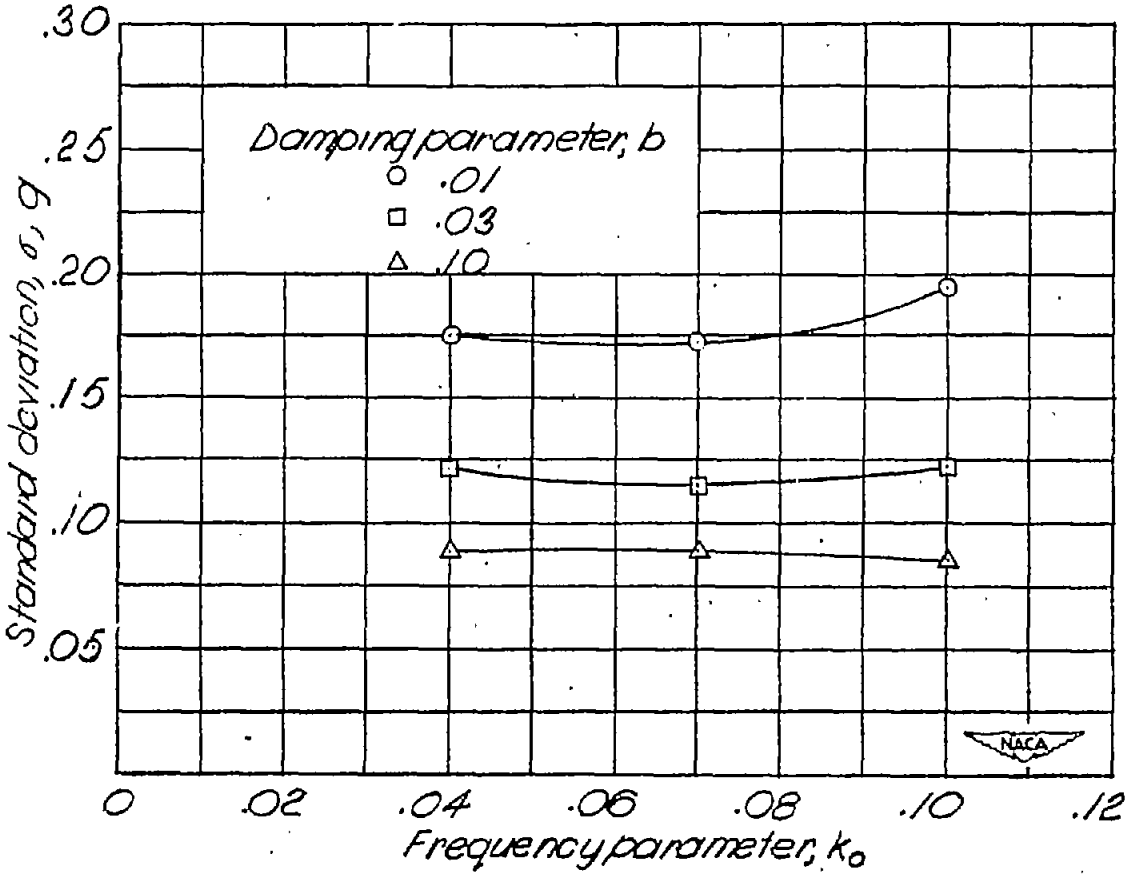


Figure 8.- Standard deviation of loads as a function of the frequency parameter $k_o$ for various values of the damping parameter b.

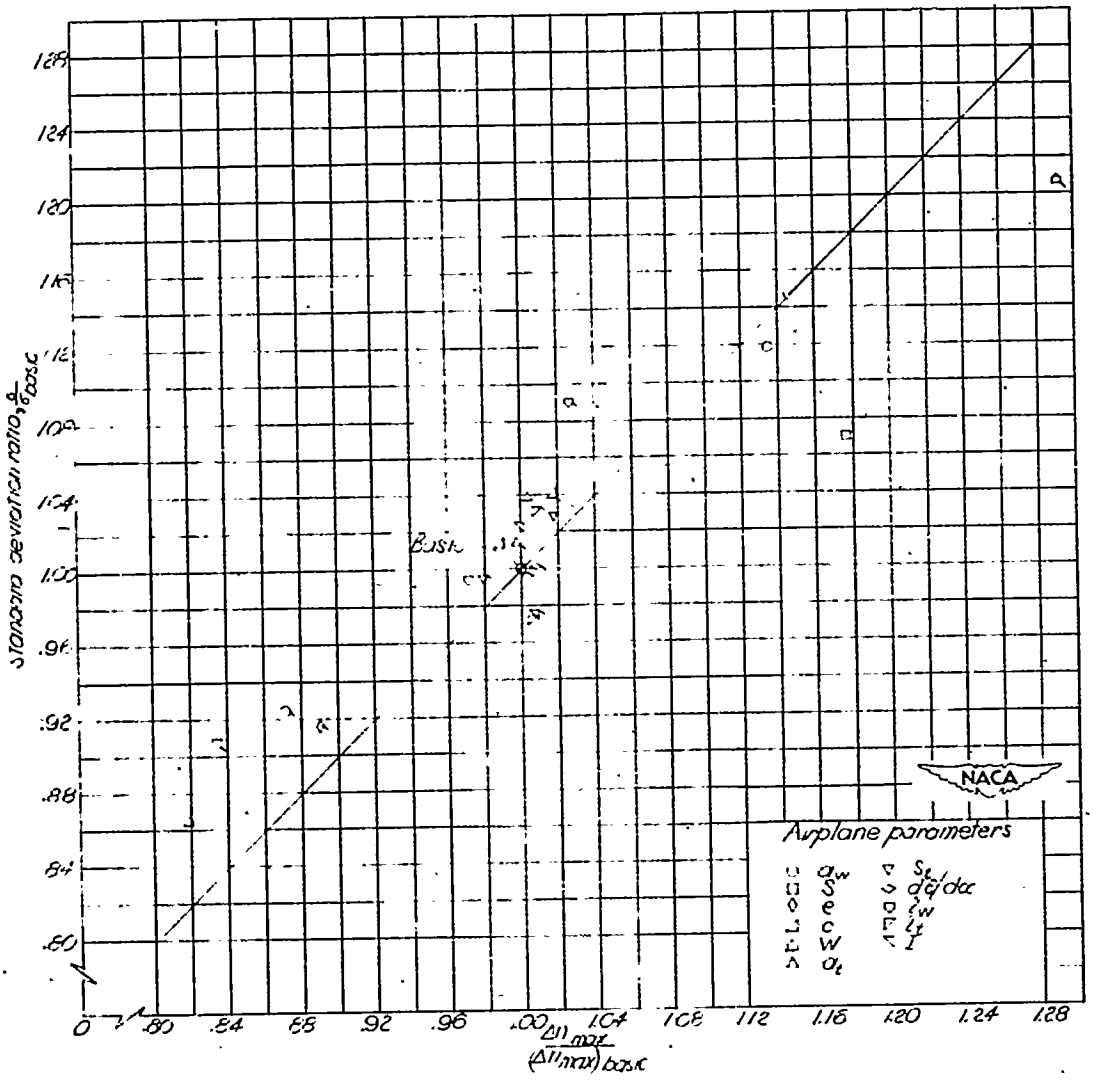


Figure 9.- Comparison of standard deviation of load with peak load response to a 10-chord-gradient triangular gust. Flagged symbols denote below-basic parameters.

NACA-Langley - 1-8-53 - 1000